

# Development of a monochromatic, uniform source facility for calibration of radiance and irradiance detectors from 0.2 $\mu\text{m}$ to 12 $\mu\text{m}$

*K. R. Lykke, P.-S. Shaw, L. M. Hanssen  
and G. P. Eppeldauer*

**Abstract.** A radiometric source facility is being constructed with narrowband, widely tuneable lasers covering the wavelength range  $\approx 200\text{ nm}$  to  $12\text{ }\mu\text{m}$ . The laser beam will pass into an integrating sphere and the output will be large-area, highly uniform, and monochromatic. This facility will be used to make a wide variety of radiometric measurements, such as radiant power, radiance, irradiance, transmittance and reflectance.

## 1. Introduction

Accurate spectral characterization and calibration of detectors requires (i) high spectral resolution, (ii) a large Lambertian source area for radiance-response calibrations, (iii) spatially uniform irradiance, and (iv) high flux levels [1, 2]. Due to the inherent limitations of methods using traditional sources, one or more of these requirements is often necessarily sacrificed. We are developing a detector-response calibration facility designed to meet all the requirements for accurate radiance and irradiance measurements. This facility (see Figure 1) incorporates custom integrating spheres to provide variable source areas with good spatial uniformity, and tuneable laser sources for high spectral resolution and high flux levels [3].

### 1.1 Source geometries for irradiance- and radiance-response measurements

Traditionally, spectral radiant power responsivities of detectors are measured with lamp-monochromator assemblies. The incident monochromatic beam underfills the detector in this mode. Different source geometries with higher input-beam power levels are needed for the calibration of irradiance and radiance meters.

In irradiance-mode calibrations, where the detectors are overfilled with a monochromatic and uniform field, the source is a point source. Our point source will be a small integrating sphere with a small exit port.

In radiance-response calibrations, a large Lambertian monochromatic source is needed. The large source

area is realized with a large exit port on a large integrating sphere.

For both irradiance- and radiance-response calibrations, the standards are irradiance detectors that are calibrated against the high-accuracy cryogenic radiometer [4]. Test irradiance detectors are calibrated against the standard detector. The radiance of the sphere exit port is calibrated against the standard irradiance detector. The radiance response of the test detector is the ratio of its electrical output signal to the known input radiance.

### 1.2 Irradiance- and radiance-level requirements

The signal level from the integrating-sphere source depends on the measurement mode, the flux transfer (between the sphere exit port and the detector), the detector type, the transmittance of the detector optics, etc.

The noise floor is different for different types of radiometers. The noise floor of a Si radiometer is about  $1\text{ fW}/(\text{Hz}^{1/2})$ . The noise floor of an InSb radiometer is about two decades higher. For a signal-to-noise ratio of 100, a radiant power of at least  $10\text{ pW}$  is needed on the InSb detector. If the aperture area in front of the detector is  $0.1\text{ cm}^2$ , the minimum irradiance requirement in the plane of the aperture is  $100\text{ pW}/\text{cm}^2$ . Roughly,  $1\text{ mW}$  radiant power is needed for the entrance port of an integrating sphere to achieve this irradiance at a distance of  $1\text{ m}$  if the exit port has a diameter of  $1\text{ cm}$ .

For radiance-response calibrations, a minimum radiance level of about  $1\text{ }\mu\text{W}/(\text{cm}^2\cdot\text{sr})$  is needed at the exit port of the sphere. This again corresponds to an input radiant power of about  $1\text{ mW}$  when the diameter of the sphere is  $20\text{ cm}$  and the diameter of the sphere exit port is  $5\text{ cm}$ .

---

K. R. Lykke, P.-S. Shaw, L. M. Hanssen and G. P. Eppeldauer:  
Optical Technology Division, National Institute of Standards  
and Technology, Gaithersburg, MD 20899, USA.

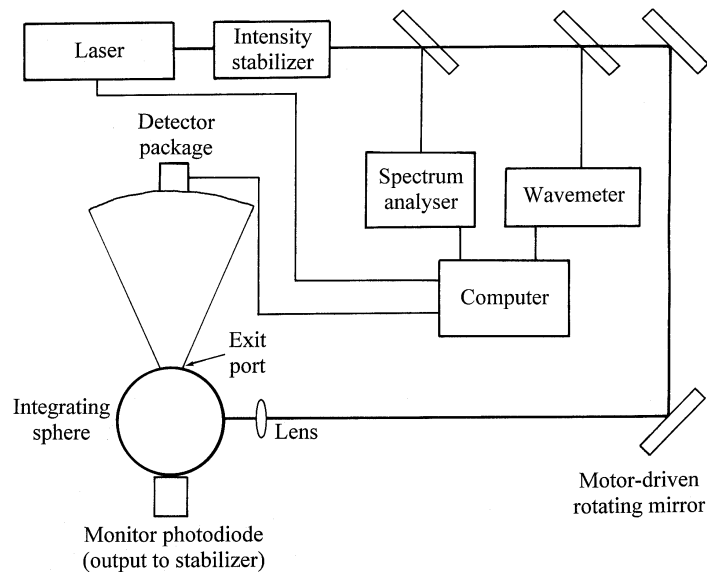


**Figure 1.** Setup for producing tuneable, monochromatic, large-area Lambertian output.

Monochromatic beams with radiant power levels of 1 mW and higher cannot be produced with traditional lamp and monochromator assemblies. The main advantages of laser sources are their much higher signal-to-noise ratio and spectral resolution compared with traditional monochromatic illuminators.

## 2. Laser systems

### 2.1 Ti-sapphire laser

The Ti-sapphire laser fundamental wavelength can be tuned over the region 670 nm to 1050 nm with the use of several sets of optics, but can cover 700 nm to 1000 nm with a single set of optics (thus facilitating rapid spectral coverage). Frequency-doubled light will cover the range 350 nm to 500 nm, frequency-tripled light 235 nm to 330 nm, and frequency-quadrupled light 200 nm to 250 nm.

When pumped with green light (an Ar-ion laser or a frequency-doubled Nd:YAG laser), a Ti-sapphire laser can either be operated in continuous-wave (cw) mode or be mode-locked to produce pulses of  $\approx 100$  fs to 10 ps duration depending on the laser configuration. The output of a mode-locked Ti-sapphire laser (repetition rate of about 100 MHz;  $\approx 1$  W average power) has a high peak power, so it is easy to generate second, third or fourth harmonics with high average power. The cw laser has a much lower peak power (about 1 W), so harmonics are much more difficult to generate. However, recent advances in build-up (Fabry-Perot) cavities and in crystal technology may enable efficient cw frequency mixing to be achieved [5-7]. The use of build-up cavities will require optical impedance matching (i.e. use of a proper input coupler for a given cavity loss to maximize output power). In addition, the input light should be single mode, so that a ring configuration will be required for the Ti-sapphire laser.

Figure 2 is a schematic diagram of the cw Ti-sapphire setup. The most unusual feature is the Littrow-mounted grating configuration for tuning the laser. Although gratings have been used for many years in cw infrared (IR) laser cavities, they have not been implemented in cw visible or near-IR cavities because of the low efficiency of most gratings. In the present setup, the grating is one of the Au-coated, holographic, very-high-efficiency versions used for pulse stretching and compressing in ultrafast studies. The first-order diffraction off this grating contains roughly 95 % of the power and is coupled back into the laser, while the zeroth-order reflection is used for output coupling. This configuration should allow continuous tuning of the output wavelength from 700 nm to 1000 nm with a relatively narrow bandwidth (and it might be possible to extend the tuning range still further by using the ultrabroadband mirrors that have recently become available [8]). For single-mode operation, the cavity can easily be configured into a ring and a unidirectional device inserted [9].

### 2.2 Nd:YAG-pumped optical parametric oscillator

The fundamental output of a Nd:YAG laser at 1064 nm can pump a lithium niobate optical parametric oscillator (OPO), but efficient birefringent phase-matching of the generated wavelengths is impossible for long crystals. However, periodic "poling" (varying the effective second-order nonlinearity) of lithium niobate (PPLN) has recently made possible extremely efficient conversion of the pump light into signal and idler radiation [10, 11]. The signal radiation can be tuned from 1.37  $\mu\text{m}$  to degeneracy at  $\approx 2.2$   $\mu\text{m}$ , while the idler tunes from degeneracy over the transparency range of lithium niobate (2.2  $\mu\text{m}$  to 4.7  $\mu\text{m}$ ). The PPLN process is so efficient that, at the powers available

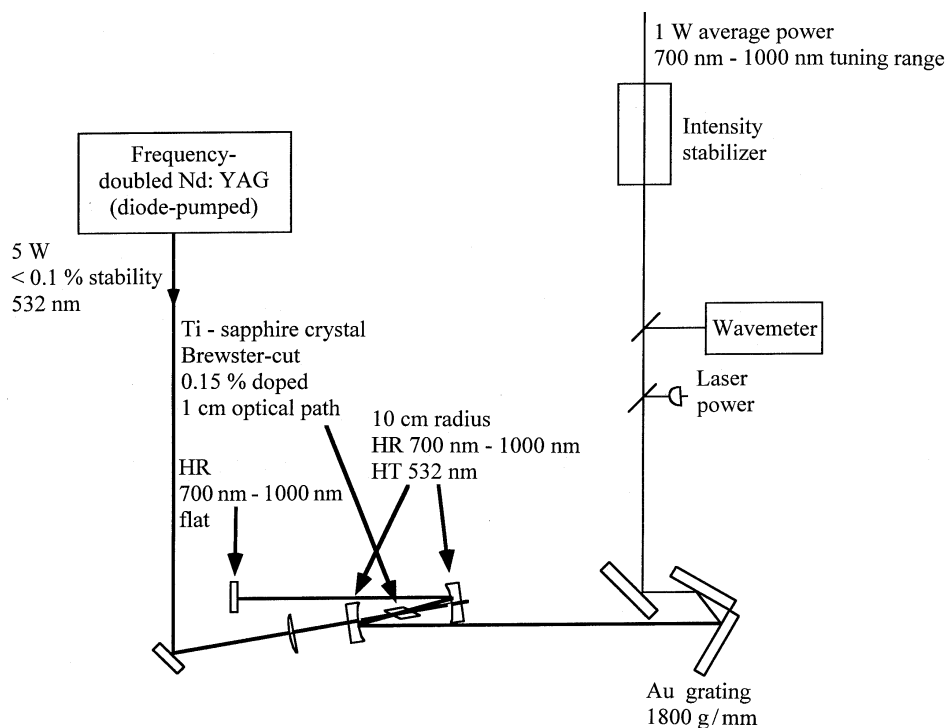


**Figure 2.** Ti-sapphire laser in its cw mode of operation. The laser is tuned by rotating the grating around an axis normal to the drawing. For the mode-locked version, the grating is replaced with an output coupler and the high-reflector end is replaced with twin fused-silica Brewster prisms for dispersion compensation. HR, high reflectivity; HT, high transmissivity.

from commercial Nd:YAG lasers, cw light can easily be converted into signal and idler beams. By using three different crystals and two sets of optics, we should be able to tune the wavelength from about 1.4  $\mu\text{m}$  to 4.7  $\mu\text{m}$ . An added feature is that the OPO is extremely narrowband for narrowband pump light. A simple cavity that has been shown by others [11] to work well is illustrated schematically in Figure 3.

This laser can also be synch-pumped and made to generate high peak powers by pumping with a mode-locked laser. We may need to use these high peak powers for generating the difference-frequency light (in  $\text{AgGaS}_2$ ) [12] from roughly 4.7  $\mu\text{m}$  to 12  $\mu\text{m}$ . These wavelengths will be generated by mixing the signal and idler waves for signal wavelengths of about 1.8  $\mu\text{m}$  to 2.0  $\mu\text{m}$  and idler wavelengths of about 2.6  $\mu\text{m}$  to 2.3  $\mu\text{m}$ . An option that may enable us to achieve an output wavelength of 20  $\mu\text{m}$  includes difference-frequency mixing in GaSe [13].

### 2.3 Ti-sapphire-pumped optical parametric oscillator

The important wavelength region between 500 nm and 700 nm can be covered by a frequency-doubled OPO driven by the Ti-sapphire laser (or cw with a dye laser). By tuning the wavelength of the Ti-sapphire pump, the signal and idler outputs of the OPO are tuned. This should enable us to fill in the spectral gaps left by the above two systems. Figure 4 shows the expected output power for the laser systems described above.

The final configuration may be somewhat different to that described here, but we believe that most of the spectral range 200 nm to 12  $\mu\text{m}$  will be covered with high power.

## 3. Integrating spheres

The laser output (typically the intensity-stabilized [14] fundamental transverse electromagnetic mode) will be directed to two detector-calibration systems, one for the ultraviolet (UV)/visible (VIS)/near-infrared (NIR) and one for the IR. The first will employ a sintered, powdered, polytetrafluoroethylene (PTFE)-coated integrating sphere that has a useful wavelength range of 0.2  $\mu\text{m}$  to 2.5  $\mu\text{m}$ . The second will have a diffuse gold-coated sphere with a range of 1  $\mu\text{m}$  to 20  $\mu\text{m}$ . The radiance of the sphere exit ports can be calibrated against standard detectors. Test radiance and irradiance detectors can be calibrated for spectral responsivities in the wavelength intervals of the different tuneable-laser sources.

## 4. Wavelength determination

For many applications, it is important to know the precise wavelengths of the radiation. We shall use a wavemeter to measure the wavelengths from 200 nm to 12  $\mu\text{m}$ . This is accomplished in the UV/VIS regions by measuring the frequency of the fundamental light (Ti-sapphire laser) and simply multiplying it for the

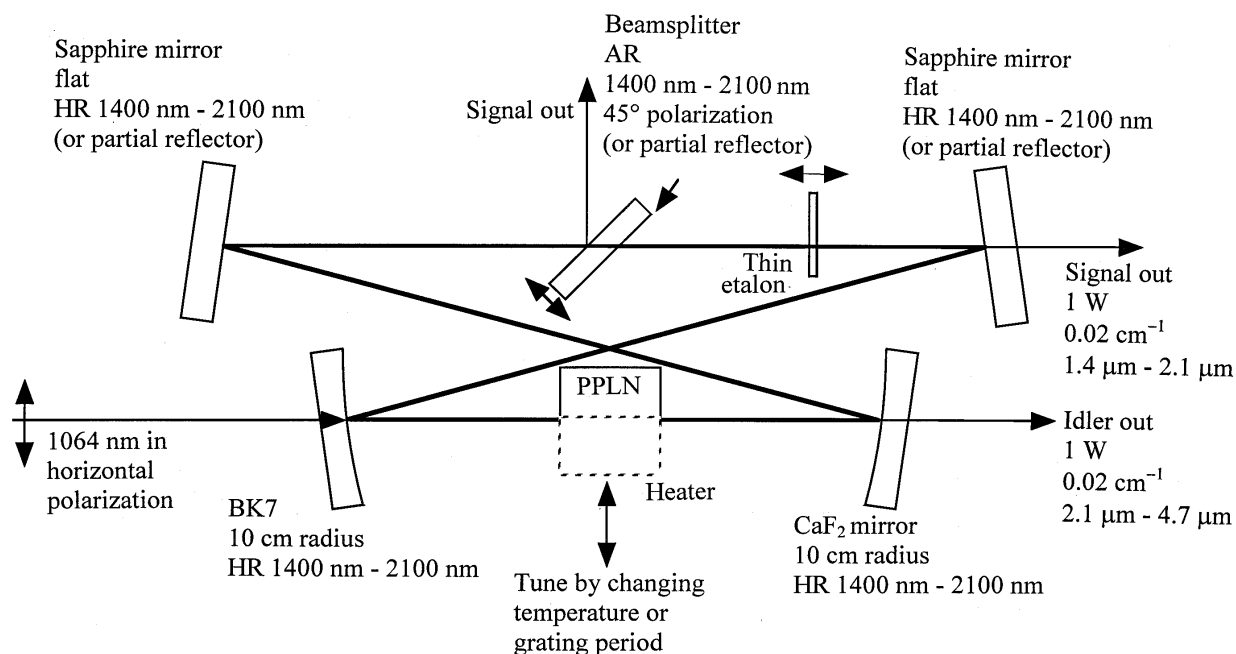


**Figure 3.** Optical parametric oscillator (OPO) for periodic poling of lithium niobate (PPLN) pumped by a cw Nd:YAG laser. The OPO is tuned by translating to a different grating period (coarse scanning), temperature tuning (medium scanning), or tilting the thin etalon (fine scanning). The idler output is from the CaF<sub>2</sub> mirror and the signal output is from either a partial reflector or the beam splitter (AR) (antireflection coating on one side). The beam splitter permits easy variation of the output coupling (from < 0.1 % to 4 %).

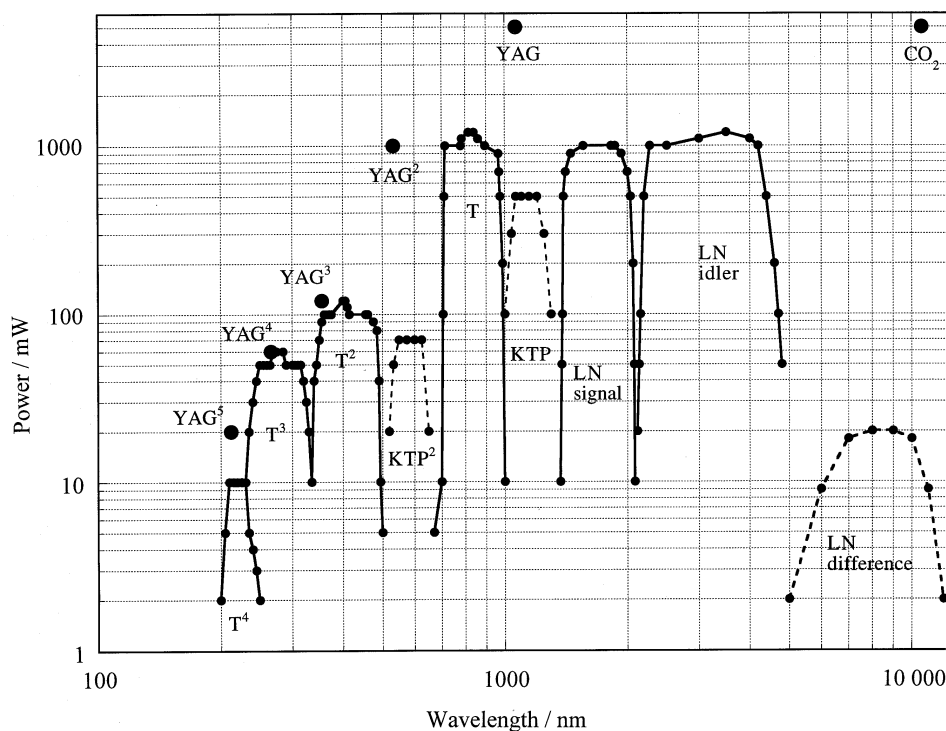


**Figure 4.** A rough plot of laser output power versus wavelength for the lasers discussed in the text. The outputs shown include Ti-sapphire fundamental (T), doubled (T<sup>2</sup>), tripled (T<sup>3</sup>) and quadrupled (T<sup>4</sup>). Also shown are the PPLN signal (LN signal), PPLN idler (LN idler) and the difference signal (LN difference). The curves labelled KTP and KTP<sup>2</sup> are the output and doubled output from a mode-locked OPO. The solid curves are for true cw output, while the dotted curves are for output that may be mode-locked (if not attained in cw mode).

frequency-doubled, -tripled, and -quadrupled beams. The wavelength of the infrared (idler) light is obtained by measuring the pump wavelength (roughly 1064 nm) and the signal wavelength (between 1.37  $\mu\text{m}$  and 2.1  $\mu\text{m}$ ). The idler wavelength (between 2.3  $\mu\text{m}$  and 4.7  $\mu\text{m}$ ) is obtained by taking the reciprocal of the difference of the reciprocals of the above two values [ $\lambda_{\text{idler}} = 1/(1/\lambda_{\text{pump}} - 1/\lambda_{\text{signal}})$ ]. The wavelength of the difference-frequency light can also be determined from the signal and idler wavelengths. The frequency (and thus wavelengths) of the Ti-sapphire-pumped OPO and its “doubled light” will be obtained in a similar manner.

## 5. Uniformity

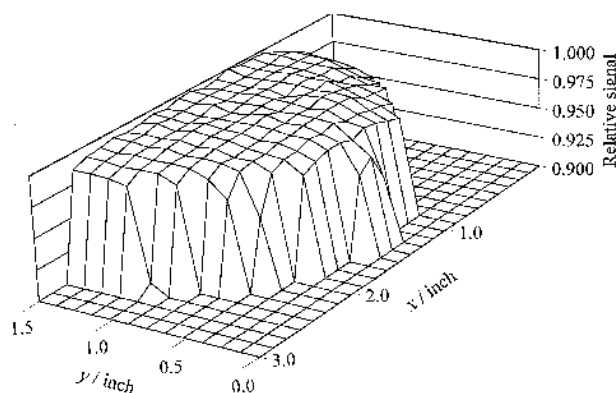
We use radiance meters [15] to map out the spatial uniformity of a 200 mm (8") diameter integrating sphere coated with Spectralon\* to be used in the UV to NIR. This sphere has variable input (irradiated with a high-power He-Ne laser for the present measurements) and output ports (one port houses a monitor diode). Part of the initial work has been to acquire a computer that incorporates a general-purpose interface bus (GPIB) board and to undertake some automation of the  $x$ ,  $y$ ,  $z$ ,  $\theta$  motions of a filter radiance meter to measure uniformity.

Figure 5 shows a uniformity plot ( $x$ ,  $y$  scan) of about half of the sphere exit port. The 632.8 nm beam was reflected off a wobbling mirror before entering the sphere in order to reduce speckle [16]. The radiance meter had a  $V(\lambda)$  filter (luminance meter) and 5 mm field-of-view. In addition, we measured the stability to be better than 0.15 % (1  $\sigma$ ) over a 2700 s, 200-point scan with the radiance meter fixed in space.

We have also measured the polarized output from the sphere for linearly polarized input light. Figure 6 shows the polarized output as a function of rotation of a  $\lambda/2$  plate (i.e. a function of the polarization of the input light). The measured variation with polarization angle can be accounted for by drift in the laser power. Since so many reflections occur inside the sphere the output light is unpolarized, which can be useful for a number of radiometric applications.

## 6. Ultraviolet operation

As UV light may damage the coating material on the integrating spheres, the long-term stability [17] of the spheres under UV irradiation is presently unknown. We need to study this effect in detail for wavelengths below 300 nm.



**Figure 5.** Three-dimensional representation of the radiance-meter detection of the output of the 200 mm (8") integrating sphere with a 64 mm (2.5") exit port. The data were obtained by computer-controlled manipulation of translation stages. The signal has been normalized and the bottom 90 % has been masked to accentuate nonuniformities. (The  $x$  and  $y$  axes are scanned in inches.)

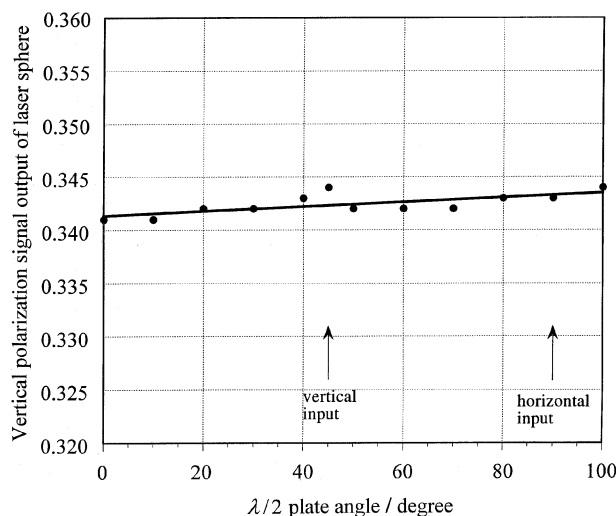


**Figure 6.** Polarized output of a 38 mm (1.5") laser sphere with 13 mm (0.5") output port obtained by varying the direction of the linearly polarized input beam with a  $\lambda/2$  plate. The drift shown by the linear least-squares fit is caused by the drift of the (unstabilized) He-Ne laser.

## 7. Conclusions

The facility discussed above is in the process of construction. We plan to have it fully operational within two years.

In addition to the uniform sources described above, widely tuneable laser outputs are useful for a number of other important radiometric purposes, such as direct calibration of detectors by scale transfer from an absolute cryogenic radiometer or trap detector [18]. Another direct use of tuneable laser sources is in highly accurate studies of transmission and reflection materials.

\* Certain commercial equipment, instruments, or materials are identified in this paper to foster understanding. Such identification does not imply recommendation or endorsement by the National Institute of Standards and Technology, nor does it imply that the materials or equipment identified are necessarily the best available for the purpose.

## References

1. Anderson V. E., Fox N. P., Nettleton D. H., Highly stable, monochromatic and tunable optical radiation source and its application to high accuracy radiometry, *Appl. Opt.*, 1992, **31**, 536-545.
2. Fox N. P., Chunnillall C. J., Harrison N. J., Hartree W. S., High-accuracy characterization and applications of filter radiometers, *Proc. SPIE*, 1996, **2815**, 32-41.
3. Gentile T. R., Cromer C. L., Mode-locked lasers for high-accuracy radiometry, *Metrologia*, 1995/96, **32**, 585-587.
4. Gentile T. R., Houston J. M., Hardis J. E., Cromer C. L., Parr A. C., National Institute of Standards and Technology high-accuracy cryogenic radiometer, *Appl. Opt.*, 1996, **35**, 1056-1068.
5. Bourzeix S., Plimmer M. D., Nez F., Julien L., Biraben F., Efficient frequency doubling of a continuous-wave titanium-sapphire laser in an external enhancement cavity, *Opt. Comm.*, 1993, **99**, 89-94.
6. Bourzeix S., de Beauvoir B., Nez F., de Tomasi F., Julien L., Biraben F., Ultraviolet light generation at 205 nm by two frequency doubling steps of a cw titanium-sapphire laser, *Opt. Comm.*, 1997, **133**, 239-244.
7. Berkeland D. J., Cruz F. C., Bergquist J. C., Sum-frequency generation of continuous-wave light at 194 nm, *Appl. Opt.*, 1997, **36**, 4159-4162.
8. Mayer E. J., Mobius J., Euteneuer A., Ruhle W. W., Szipocs R., Ultrabroadband chirped mirrors for femto-second lasers, *Opt. Lett.*, 1997, **22**, 528-530.
9. Lykke K. R., Murray K. K., Lineberger W. C., Threshold photodetachment of H<sup>-</sup>, *Phys. Rev. A*, 1991, **43**, 6104-6107.
10. Myers L. E., Eckardt R. C., Fejer M. M., Byer R. L., Bosenberg W. R., Pierce J. W., Quasi-phase-matched optical parametric oscillators in bulk periodically poled LiNbO<sub>3</sub>, *J. Opt. Soc. Am. B*, 1995, **12**, 2102-2116.
11. Bosenberg W. R., Drobshoff A., Alexander J. I., Myers L. E., Byer R. L., 93 % pump depletion, 3.5 W continuous-wave, singly-resonant optical parametric oscillator, *Opt. Lett.*, 1996, **21**, 1336-1338.
12. Kato K., High-power difference-frequency generation at 5-11  $\mu\text{m}$  in AgGaS<sub>2</sub>, *IEEE J. Quantum Electron.*, 1984, **QE-20**, 698-699.
13. Suhre D. R., Singh N. B., Balakrishna V., Fernelius N. C., Hopkins K. K., Improved crystal quality and harmonic generation in GaSe doped with indium, *Opt. Lett.*, 1997, **22**, 775-777.
14. Fowler J. B., Lind M. A., Zalewski E. F., A servo-controlled electro-optic modulator for cw laser power stabilization and control, *Natl. Bur. Stand. Tech. Note* 987, 1979.
15. Eppeldauer G., Near Infrared Standards, *Proc. SPIE*, 1996, **2815**, 42-54.
16. Mielenz K. D., Saunders R. D., Shumaker J. B., Spectroradiometric determination of the freezing temperature of gold, *J. Res. Natl. Inst. Stand. Technol.*, 1990, **95**, 49-67.
17. Gibbs D. R., Duncan F. J., Lambe R. P., Goodman T. M., Ageing of materials under intense ultraviolet radiation, *Metrologia*, 1995/96, **32**, 601-607.
18. Gentile T. R., Houston J. M., Cromer C. L., Realization of a scale of absolute spectral response using the NIST high-accuracy cryogenic radiometer, *Appl. Opt.*, 1996, **35**, 4392-4403.

---

*Metrologia*, 1998, **35**, 479-484.

## Page 484:

Comment from the Editor.

Owing to an unfortunate printing error, the final page of this article by Dr Lykke *et al.* was printed blank in the special NEWRAD issue **35**(4). The complete article is reprinted here, with apologies to all concerned.

---